IEEE Access
Multidisciplinary | Rapid Review | Open Access Journal

Received March 10, 2018, accepted April 1, 2018, date of publication April 6, 2018, date of current version May 16, 2018.

Digital Object Identifier 10.1109/ACCESS.2018.2823765

Analog Circuit Incipient Fault Diagnosis Method Using DBN Based Features Extraction

CHAOLONG ZHANG[1,2], YIGANG HE[2], LIFENG YUAN[3], AND SHENG XIANG[3]

[1]School of Physics and Electronic Engineering, Anqing Normal University, Anqing 246011, China
[2]School of Electrical Engineering, Wuhan University, Wuhan 430072, China
[3]School of Electrical Engineering and Automation, Hefei University of Technology, Hefei 230009, China

Corresponding authors: Chaolong Zhang (zhangchaolong@126.com) and Yigang He (18655136887@163.com)

This work was supported in part by the National Natural Science Foundation of China under Grant 51607004 and Grant 51577046, in part by the State Key Program of National Natural Science Foundation of China under Grant 51637004, in part by the National Key Research and Development Plan "Important Scientific Instruments and Equipment Development" under Grant 2016YFF0102200, in part by the Equipment Research Project in Advance under Grant 41402040301, and in part by the Anhui Provincial Natural Science Foundation under Grant 1608085QF157.

ABSTRACT Correct identifying analog circuit incipient faults is useful to the circuit's health monitoring, and yet it is very hard. In this paper, an analog circuit incipient fault diagnosis method using deep belief network (DBN) based features extraction is presented. In the diagnosis scheme, time responses of analog circuits are measured, and then features are extracted by using the DBN method. Meanwhile, the learning rates of DBN are produced by using quantum-behaved particle swarm optimization (QPSO) algorithm, which is beneficial to optimizing the structure parameters of DBN. Afterward, a support vector machine (SVM) based incipient fault diagnosis model is constructed on basis of the extracted features to classify incipient faulty components, where the regularization parameter and width factor of SVM are yielded by using the QPSO algorithm. Sallen–Key bandpass filter and four-op-amp biquad high pass filter incipient fault diagnosis simulations are conducted to demonstrate the proposed diagnosis method, and comparisons verify that the proposed diagnosis method can produce higher diagnosis accuracy than other typical analog circuit fault diagnosis methods.

INDEX TERMS Analog circuits, incipient fault diagnosis, DBN, SVM, QPSO.

I. INTRODUCTION

Circuits are widely used in domestic appliances, automotive electronics, power supply systems, and industrial electronics, etc [1]–[6]. Generally, circuits are divided into analog and digital circuits. Meanwhile, 80% circuit faults occur in the analog circuits although there are less than 20% of circuits are analog [7]. As a result, analog circuit fault diagnosis plays an important role in the health monitoring of circuits.

In general, analog circuit faults are categorized into hard faults and soft faults. Hard faults refer to the circuit components' catastrophic failures such as open circuit and short circuit, and they are easy to be recognized. Soft faults denote the component values' deviations, and they occur most frequently in the circuit operation. Obviously, soft faults are more difficult to be diagnosed than hard faults, and analog circuit fault diagnosis generally refers to the soft fault diagnosis.

In order to indentify analog circuit faults, many researchers have made contributions in recent years [7]–[25]. Spina and Upadhyaya [8] have applied the measured time responses to an artificial neural network (ANN) directly, where a large number of invalid information contained in the time responses not only has brought about high computational load, but also has leaded to poor results. Therefore, extracting efficient features from the measured signals has been a critical research area in analog circuit fault diagnosis because the efficient features can reflect significant differences between different faults. Aminian *et al.* [9]–[12] have introduced wavelet transform to process the measured signals, and wavelet coefficients have been extracted as features. Tan *et al.* [13] have presented S-transform to deal with the raw data, and the magnitudes of S-transform's output have been used as features. Yuan *et al.* [14] have calculated kurtosis and entropy of the measured signals, and have applied them as features to the diagnosis. Wavelet-based fractal analysis has been presented by Xiao and Feng [15], and it has been applied to decompose the measured signal data into fractal dimensions used as features. Particle swarm optimization (PSO) algorithm and Mahalanobis distance have

been used by Long *et al.* [25] to select near-optimal features. However, it is unavoidable to generate a large amount of redundant information by using traditional features extraction methods. In order to remove the redundant information contained in the extracted features and reduce the dimensionality of the features, principle components analysis is used in most of the works to generate principle components from the extracted features [9]–[12], [15], [16], which further complicates the features extraction process.

In order to monitor the analog circuit's health degradation and predict its failure time, it is necessary to correctly identify analog circuit faults at their incipient stages. Analog circuit incipient faults refer to that the circuit components' value deviations have been out of their tolerance ranges while the values have not yet developed to their fault values. Meanwhile, the components tend to be faulty. However, most of the diagnosis works focus on analog circuit fault diagnosis [8]–[22], rather than incipient fault diagnosis [23]–[25]. The reason is that the extracted features are difficult to reflect the sufficiently discriminative information of incipient faults because the differences between the different incipient fault values and nominal value are too small. Moreover, the overlapping of different incipient faults occurs easily. Therefore, it is critically important to develop efficient features extraction method to extract essential features for analog circuit incipient fault diagnosis.

Recently, deep belief network (DBN) has been proposed as an unsupervised features extraction method because the DBN method can efficiently extracts high-level and hierarchical features from the measured signal data by using a multiple nonlinear transformation [26]. Compared to the traditional signal-based features extraction methods, DBN directly extracts features from signals without applying any prior domain knowledge. Hence, signals from the same source are equally processed as uniform high-order representations. In recent years, DBN has been applied to extract features for visual recognition, phone recognition and spectral–spatial classification [27]–[29], and promising results are obtained.

DBN's learning rates affect its features extraction effectiveness deeply because the learning rates determine the DBN's structure parameters. However, the learning rates are set according to experience traditionally because the DBN method is lack of theory dependence, which is hard to obtain the optimal values. Furthermore, the learning rates need to be reset their values when the measured signal data change. As a result, it is necessary to develop a method to generate the optimal values for the DBN's learning rates automatically based on the measured signal data.

With respect to the diagnosis tool used in the diagnosis, ANN has been a classical method applied in analog circuit fault diagnosis [8]–[16]. However, the method has disadvantages of low convergence rate, poor generalization performance and easy falling local optimal solution. Support vector machine (SVM) [30] accounts for the trade-off between learning ability and generalizing ability by minimizing structure risk, and the method has demonstrated good learning and generalization performance for small sample [17]–[22], which is applicable for analog circuit fault diagnosis. Therefore, SVM has been used to construct diagnosis model for the purpose of classifying analog circuit faults [17]–[22]. Meanwhile, regularization parameter and width factor are important parameters in the SVM, and they need to be set optimal values when constructing the SVM based diagnosis model.

Quantum-behaved particle swarm optimization (QPSO) algorithm is a heuristic optimizing method based on quantum theory and PSO algorithm [31], [32], and it can seek suitable parameters for complex, nonlinear and multimodal problems [33]–[35]. In this paper, an analog circuit incipient fault diagnosis method using DBN based features extraction, SVM and QPSO is presented. In the incipient fault diagnosis scheme, different incipient fault modes of analog circuits are set firstly, and then time responses of analog circuits are measured. Afterwards, the DBN method is used to extract the hierarchical representations of time responses as features, where the learning rates of DBN are generated by QPSO algorithm. Based on the extracted features, a SVM based diagnosis model is constructed, where the regularization parameter and width factor of SVM are also generated by QPSO algorithm. Finally, the constructed incipient fault diagnosis model is used to identify analog circuit incipient faults.

The material in the paper is organized in the following order: Section 2 briefly presents the DBN based features extraction method. Section 3 introduces SVM algorithm. Section 4 describes QPSO algorithm, and discusses parameters generation procedure. Analog circuit incipient fault diagnosis simulations are implemented in Section 5. Finally, Section 6 draws conclusions.

II. DBN BASED FEATURES EXTRACTION METHOD

Features extraction is critically important to incipient fault diagnosis because the efficient features are beneficial to improving the diagnosis accuracy. As a result, various techniques have been used to extract features for fault diagnosis. Especially, DBN based features extraction method is presented to address this challenging problem.

DBN is a typical deep learning method. The method employs a greedy layer-wise training model in its pretraining phase firstly, and then adopts a back-propagation in subsequent fine-tuning phase. In the work, DBN is utilized to extract efficient features for analog circuit incipient fault diagnosis.

A. RESTRICTED BOLTZMAN MACHINE (RBM)

RBMs construct DBN by a greedy layer-wise training model. RBM is a two-layer network which includes a visible layer $\boldsymbol{v} = \{0, 1\}^D$ and a hidden layer $\boldsymbol{h} = \{0, 1\}^K$, and its architecture is showed in Fig. 1. Visible layer and hidden layer both contain a number of units and the input data are fed to the visible layer $\boldsymbol{v}$ generally. The energy of the layers' joint

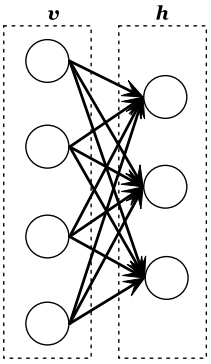

FIGURE 1. RBM's architecture.

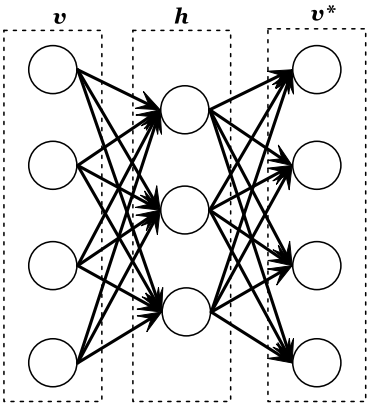

FIGURE 2. RBM reconstruction procedure.

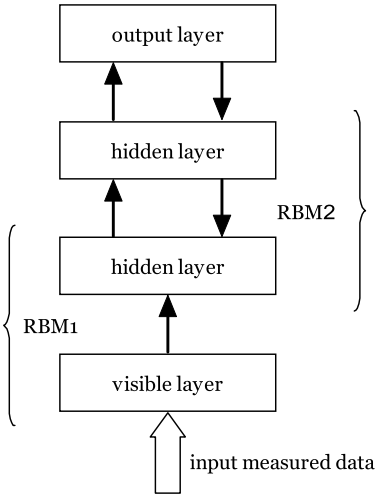

FIGURE 3. A typical instance of DBN.

configuration is defined as

$$E(\boldsymbol{v},\boldsymbol{h}) = -\sum_{i=1}^{D}\sum_{j=1}^{K} v_i w_{ij} h_j - \sum_{i=1}^{D} c_i v_i - \sum_{j=1}^{K} b_j h_j \quad (1)$$

where w_{ij} is the weight associate with visible unit i and hidden unit j; c_i is a bias term of visible unit i; b_j is a bias term of hidden unit j. In DBN, weights are important structure parameters.

The layers' joint distribution is given by

$$p(\boldsymbol{v},\boldsymbol{h}) = \frac{1}{Z}\exp(-E(\boldsymbol{v},\boldsymbol{h})) \quad (2)$$

where Z is a normalizing constant. Reducing the energy can increase the probability.

The hidden layer $\boldsymbol{h}$'s and visible layer $\boldsymbol{v}$'s conditional distributions are generated as follows

$$p(h_j = 1|\boldsymbol{v}) = \sigma(\sum_i w_{ij} v_i + b_j) \quad (3)$$

$$p(v_i = 1|\boldsymbol{h}) = \sigma(\sum_j w_{ij} h_j + c_i) \quad (4)$$

$$\sigma(s) = \frac{1}{1+\exp(-s)} \quad (5)$$

By setting each v_i to 1 in (4), the visible layer is reconstructed.

Weights are updated by using contrastive divergence method. A weight's variation is defined as

$$\Delta w_{ij} = \varepsilon(v_i h_{jdata} - v_i h_{jreconstrction}) \quad (6)$$

where ε is a learning rate. Every RBM has a learning rate and proper values of weights can be generated by a suitable learning rate.

RBM reconstruction procedure is showed in Fig. 2. In the procedure, the hidden layer $\boldsymbol{h}$ tries to reconstruct a visible layer $\boldsymbol{v}^*$ which is almost the same with the visible layer $\boldsymbol{v}$. Then, the data contained in hidden layer $\boldsymbol{h}$ are extracted as features. If the RBN model can recover the visible layer perfectly, it represents that the hidden layer $\boldsymbol{h}$ learns effective information from the input data, and the produced weights can be regarded as good structure parameters of the input data. Therefore, the learning rate is important to the RBM reconstruction procedure for it can determine the DBN's structure parameters.

B. DBN AND ITS FEATURES EXTRACTION PROCEDURE

Usually, only a RBM can not learn features well. Therefore, more than one RBM are stacked to extract features. The extracted features of the first RBM are input to the next RBM. Fig. 3 shows a typical instance of a DBN with two RBMs, where ↑ refers to pretraining, and ↓ denotes fine-tuning; the output layer employs a Softmax classifier usually.

The DBN based features extraction method includes two training phases: pretraining phase and fine-tuning phase. In the pretrainning phase, the input signal data are learnt by the first RBM and the first layer's features are produced. Then, the first layer's features are input to the second RBM and the second layer's features are generated. Repeatedly run in the manner, and the features of last RBM are the learnt features of pretrainning phase. Then, the features of last RBM are input to the output layer for fine-tuning.

In the fine-tuning phase, the pretrained DBN network is fine-tuned by a Softmax classifier. This Softmax classifier

classifies the learned features of pretrainning phase. The input data labels are compared with the labels generated by the Softmax classifier, and then a back-propagation is performed to minimize errors by refining the weights. After fine-tuning, the updated weights are used in the RBM, and the new learnt features of last RBM are the extracted features of DBN finally.

During the DBN based features extraction procedure, the learning rates are critically important to the DBN. In the past works [27]–[29], the learning rates are set according to experience, which is inefficient and easy to miss the optimal values. In the work, QPSO algorithm is used to produce suitable values for the learning rates.

III. SVM

An incipient fault diagnosis model needs to be constructed after features extraction. SVM is a commonly used classifier in analog circuit fault diagnosis because of its learning and generalization performance for small sample. In the work, the SVM is used to set up a diagnosis model based on the extracted features.

The SVM is statistical learning technique which explores an optimal hyperplane as a decision function in high-dimensional space. Assume $\mathrm{D} = \{\mathbf{x}_i, y_i\}_{i=1}^{N}$ is a labeled data set, where $\mathbf{x}_i \in \mathrm{R}^d$ and $y_i \in \{1, -1\}$. These training patterns are linearly separable if the following condition is satisfied

$$y_i(\mathbf{w} \cdot \mathbf{x}_i + b) - 1 \geq 0 \tag{7}$$

where $\mathbf{w}$ and b are parameters with $\mathbf{w} \in \mathrm{R}^d$ and $b \in \mathrm{R}$.

In supervised learning, a hypothesis f needs to be generated by

$$f_{\mathbf{w},b}(\mathbf{x}) = sign(\mathbf{w} \cdot \mathbf{x} + b) \tag{8}$$

The SVM seeks the separating hyperplanes for the distance of classes by maximizing a line perpendicular to the hyperplane. A constrained optimization problem is presented as follow

$$\min_{\mathbf{w},b} \quad \frac{1}{2} \|\mathbf{w}\| \tag{9}$$

A positive constant C called regularization parameter is introduced to balance the margin and misclassification error. Therefore, problem (9) can be rewritten as

$$\min_{\mathbf{w},b,\xi_1,\ldots\xi_N} \left[C \sum_{i=1}^{N} \xi_i + \frac{1}{2} \|\mathbf{w}\| \right] \tag{10}$$

where $\zeta_i \geq 0$, and it is a slack variable.

$K(\mathbf{x}, \mathbf{x}_i) = \boldsymbol{\varphi}(\mathbf{x}) \cdot \boldsymbol{\varphi}(\mathbf{x}_i)$ is introduced to map the original input space to a Hilbert space H and the decision function can be represented by

$$f(\mathbf{x}) = sign(\sum_{i} \lambda_i y_i K(\mathbf{x}, \mathbf{x}_i) + b) \tag{11}$$

where λ_i is a Lagrange multiplier.

Gaussian radial basis function is a commonly used kernel function with powerful nonlinear processing capability

$$K(\mathbf{x}, \mathbf{x}_i) = \exp(-\frac{(\mathbf{x} - \mathbf{x}_i)^2}{2\gamma^2}) \tag{12}$$

where γ is a width factor.

The regularization parameter and width factor of SVM are important to the classification. In the work, QPSO algorithm is adopted to generate the parameters.

IV. QPSO ALGORITHM AND ARAMETERS OPTIMIZATION PROCEDURE

A. QPSO ALGORITHM

PSO algorithm is a heuristic searching method presented by Eberhart and Kennedy in 1995 [32]. By impersonating birds' fishing procedure, particles in the algorithm are employed to explore the optimal solution for the optimization problem. However, the algorithm has shortcomings of easy trapping in local optimum and slow convergence. Sun *et al.* [31] have proposed QPSO algorithm based on quantum theory. The probability of each particle's next iteration position relies on the potential field of the particle, which is defined as follows

$$X_i(t+1) = P \pm a|nbest - X_i(t)|\mathrm{In}(\frac{1}{u}) \tag{13}$$

$$nbest = \frac{1}{N} \sum_{i=1}^{N} P_i \tag{14}$$

$$P = sP_i + (1-s)P_g \tag{15}$$

where $i = 1, 2, \cdots, N$, and N is swarm size; u and s are uniformly distributed random numbers generated between 0 and 1; P_g is the global optimal position of all particles and P_i is the particle i's optimal position; $X_i(t+1)$ is the position of particle i in iteration $t+1$; $nbest$ is the center of all individual optimal positions; a is a contraction expansion coefficient.

Assume $f(x)$ is a maximized fitness function, and the particle i's optimal position is defined as

$$P_i = \begin{cases} P_i, f(P_i) > f(X_i(t+1)) \\ X_i(t+1), f(P_i) \leq f(X_i(t+1)) \end{cases} \tag{16}$$

The global optimal position is determined by

$$P_g(t) = \arg\max \{f(P_i)\} \tag{17}$$

QPSO algorithm has already been used for solving various optimization problems, and promising results have been obtained [33]–[35]. In the work, QPSO algorithm is employed to generate the appropriate learning rates for DBN and produce the suitable regularization parameter and width factor for SVM.

B. PROCEDURE OF PARAMETERS GENERATION

In DBN, every RBM has a learning rate. Traditionally, the learning rates are set according to experience. In the work, the learning rates are generated by QPSO algorithm based on the measured signal data. Every learning rate corresponds to

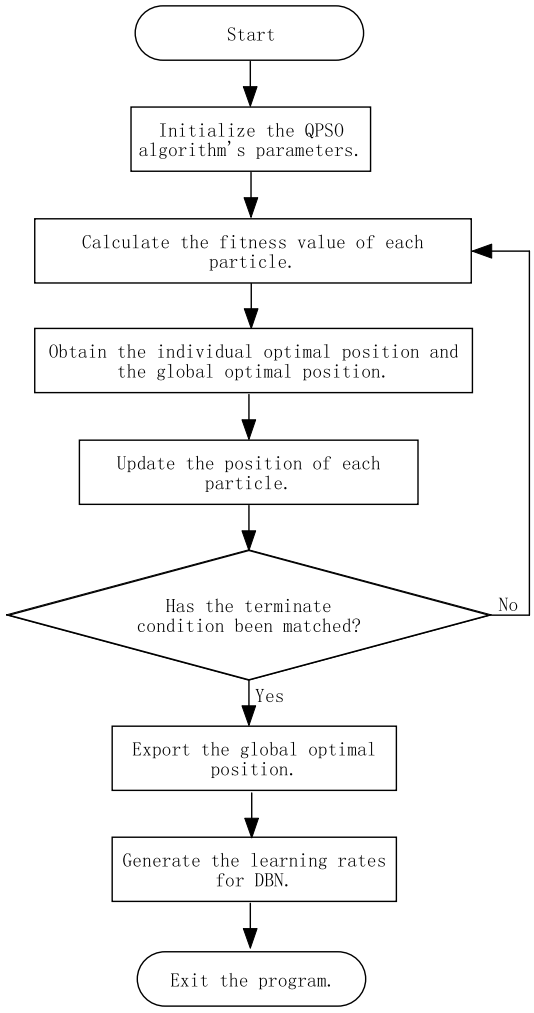

FIGURE 4. Flowchart of learning rates generation by using QPSO algorithm.

one dimension in the multi-dimensional position of a particle. The flowchart of the learning rates generation is showed in Fig. 4 and the generation steps are described as follows

1) Initialize the QPSO algorithm's parameters including maximum iteration, swarm size, contraction expansion coefficient, and each particle's position, etc.

2) Calculate the fitness value of each particle, and the steps can be described as follows

2.1) Map the multi-dimensional position of a particle to the learning rates of a DBN, and then extract the features by using the DBN.

2.2) Perform incipient fault diagnosis by using the DBN's Softmax classifier based on the extracted features, and then diagnosis accuracy is obtained as following

$$diagnosis\ accuracy = \frac{S_{correct}}{S_{total}} \times 100\% \qquad (18)$$

where S_{total} refers to the total amount of training data, and $S_{correct}$ denotes the number of training data classified correctly.

2.3) Export the diagnosis accuracy as the particle's fitness value.

3) Yield each particle's optimal position and elect the global optimal position according to (16) and (17).

4) Update the position of each particle in accordance with (13) - (15).

5) Repeat step 2) to 4) until matching the terminate condition.

6) Export the optimal multi-dimensional position generated in the optimization as the learning rates of DBN.

7) Exit the program.

The regularization parameter and width factor of SVM are generated by QPSO algorithm based on the extracted features, and the two parameters are mapped to the 2-dimensional position of each particle. Diagnosis accuracy produced by the SVM based on the extracted features is used as the fitness function. The generation steps are described as follows

1) Initialize the QPSO algorithm's parameters including the maximum iteration, swarm size, contraction expansion coefficient, and each particle's position, etc.

2) Calculate the fitness value of each particle, and the steps can be described as follows

2.1) Map the 2-dimensional position of a particle to the regularization parameter and width factor of a SVM, respectively.

2.2) Perform incipient fault diagnosis by using the SVM based on the extracted features, and then diagnosis accuracy is obtained according to (18).

2.3) Export the diagnosis accuracy as the particle's fitness value.

3) Calculate each particle's optimal position and elect the global optimal position according to (16) and (17).

4) Update the position of each particle in accordance with (13) - (15).

5) Repeat step 2) to 4) until matching the terminate condition.

6) Export the optimal 2-dimensional position generated in the optimization as the regularization parameter and width factor of SVM.

7) Exit the program.

V. SIMULATION EXPERIMENTS

The occurrence of single-fault condition has higher probability than the double-fault condition, and the method applying to the single-fault condition is also applicable for the double-fault condition [15, 20]. As a result, the single-fault condition is considered in the work to demonstrate the proposed analog circuit incipient fault diagnosis method.

A. EXAMPLE CIRCUITS

Sallen–Key bandpass filter and four-opamp biquad highpass filter circuits are commonly used experiment circuits in the diagnosis works [8]–[17], [19]–[21], [23], [25]. They are also used as experiment circuits in the work for the purpose of verifying the performance of the presented method conveniently.

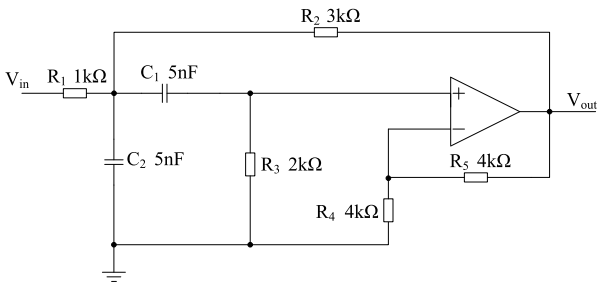

FIGURE 5. Schematic of Sallen–Key bandpass filter circuit.

TABLE 1. Incipient fault codes, incipient fault classes, nominal values and incipient fault values for bandpass filter.

Incipient fault code	Incipient fault class	Nominal value	Incipient fault value
F0	NF	-	-
F1	$R_2\uparrow$	3 kΩ	3.75 kΩ
F2	$R_2\downarrow$	3 kΩ	2.25 kΩ
F3	$R_3\uparrow$	2 kΩ	2.5 kΩ
F4	$R_3\downarrow$	2 kΩ	1.5 kΩ
F5	$C_1\uparrow$	5 nF	6.25 nF
F6	$C_1\downarrow$	5 nF	3.75 nF
F7	$C_2\uparrow$	5 nF	6.25 nF
F8	$C_2\downarrow$	5 nF	3.75 nF

Example 1—Sallen–Key bandpass filter: The circuit showed in Fig. 5 is used as the first example circuit. Through component sensitivity analysis, R_2, R_3, C_1 and C_2 are considered as critical components for they have more effects on the center frequency of circuit. Hence, these components are selected as experiment components. Generally, a component of analog circuit is considered to be faulty when its value has been deviated from its nominal value about 50%. Hence, the component with a 25% deviation from its nominal value is considered to be an incipient fault in the work. The faulty time responses are processed in order to form 9 different incipient fault classes including $R_2\uparrow$, $R_2\downarrow$, $R_3\uparrow$, $R_3\downarrow$, $C_1\uparrow$, $C_1\downarrow$, $C_2\uparrow$, $C_2\downarrow$ and no fault (NF), where $\uparrow$ and $\downarrow$ refer to higher and lower than the nominal value, respectively. Incipient fault codes, incipient fault classes, nominal and incipient fault component values are showed in Table 1.

Example 2—four-opamp biquad highpass filter: This circuit showed in Fig. 6 is more complex. R_1, R_2, R_3, R_4, C_1 and C_2 are considered as critical components through component sensitivity analysis. The measured time responses are processed to form 13 incipient fault classes including $R_1\uparrow$, $R_1\downarrow$, $R_2\uparrow$, $R_2\downarrow$, $R_3\uparrow$, $R_3\downarrow$, $R_4\uparrow$, $R_4\downarrow$, $C_1\uparrow$, $C_1\downarrow$, $C_2\uparrow$, $C_2\downarrow$ and NF. Incipient fault codes, incipient fault classes, nominal and incipient fault component values are showed in Table 2.

B. SIMULATION PROCEDURE

In the incipient fault diagnosis scheme, a single pulse of height 10v with duration of 10us is used as the circuit input. Time responses are measured by sampling the outputs of circuits. 120 samples for each incipient fault class are produced. Then, the sample data are divided into training data and testing data equally and randomly. The overall simulation

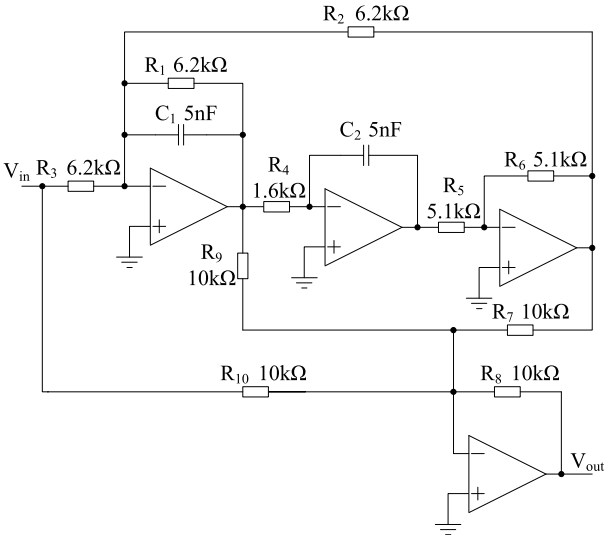

FIGURE 6. Schematic of four-op-amp biquad highpass filter circuit.

TABLE 2. Incipient fault codes, incipient fault classes, nominal values and incipient fault values for highpass filter.

Incipient fault code	Incipient fault class	Nominal value	Incipient fault value
F0	NF	-	-
F1	$R_1\uparrow$	6.2kΩ	7.75kΩ
F2	$R_1\downarrow$	6.2kΩ	4.65kΩ
F3	$R_2\uparrow$	6.2kΩ	7.75kΩ
F4	$R_2\downarrow$	6.2kΩ	4.65kΩ
F5	$R_3\uparrow$	6.2kΩ	7.75kΩ
F6	$R_3\downarrow$	6.2kΩ	4.65kΩ
F7	$R_4\uparrow$	1.6kΩ	2kΩ
F8	$R_4\downarrow$	1.6kΩ	1.2kΩ
F9	$C_1\uparrow$	5nF	6.25nF
F10	$C_1\downarrow$	5nF	3.75nF
F11	$C_2\uparrow$	5nF	6.25nF
F12	$C_2\downarrow$	5nF	3.75nF

procedure is showed in Fig. 7, and the detailed diagnosis steps are described as follows

1) Measure time responses as sample data for each incipient fault class.

2) The measured data are divided into training data and testing data. The training data are employed to train a DBN to extract features and then construct a diagnosis model, and the testing data are applied to test the performance of the diagnosis method.

3) The training data are used as the input of DBN. DBN extracts deep and inherent features from the input data, where the learning rates of DBN are generated by QPSO algorithm.

4) A SVM based diagnosis model is constructed by using the extracted features, and the SVM's regularization parameter and width factor are generated by QPSO algorithm.

5) The diagnosis model is tested based on the features generated by the DBN and testing data.

6) Output the diagnosis accuracy of the testing data.

C. SIMULATION RESULTS AND ANALYSIS

The following two cases are conducted in the simulation experiment.

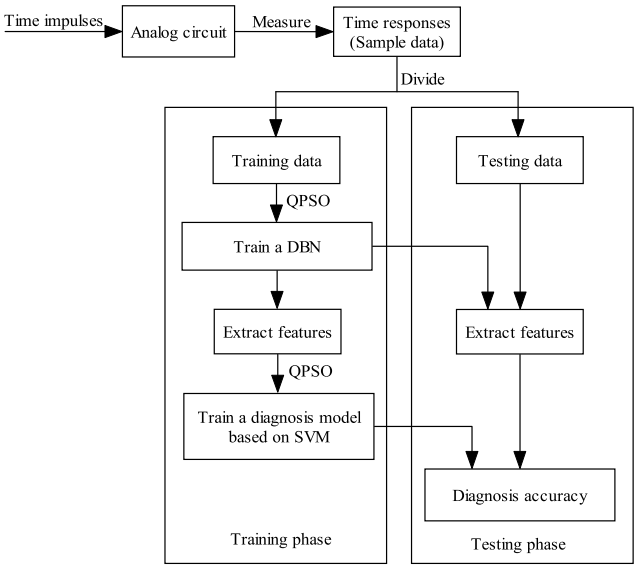

FIGURE 7. Simulation procedure.

TABLE 3. The two cases' learning rates generated by QPSO algorithm.

Case	Learning rate 1	Learning rate 2
Case 1	0.283509250924758	0.271132638924804
Case 2	0.044994542976916	0.035064909557063

Case 1: Sallen–Key bandpass filter circuit incipient fault diagnosis.

Case 2: Four-op-amp biquad highpass filter circuit incipient fault diagnosis.

The measured time response data are 100-dimensional, and they are directly fed to the bottom visible layer of DBN. The structure of DBN with two hidden layers is classical for the structure has the lowest computational cost and reasonable performance. Therefore, the structure is used in the simulation. The numbers of units of the first and second hidden layer are set to 50 and 25, respectively. The visible layer and the first hidden layer constitute the first RBM, and the first and second hidden layers form the second RBM.

Traditionally, the learning rates of DBN are set empirically [26]–[29]. In the work, the learning rates of DBN are generated by using QPSO algorithm. The QPSO algorithm's swarm size and the maximum iteration are set to 10 and 100, respectively; the contraction expansion coefficient decreases from 1 to 0.3 with the iteration. When the diagnosis accuracy reaches 100% or the iteration reaches its maximum in the training phase, the generation procedure is terminated.

Table 3 shows the generated learning rates of two cases. The generation procedure of case 1 is only five iteration for the diagnosis accuracy reaches 100% in the fifth iteration. The generation procedure of case 2 is demonstrated in Fig. 8. As can be seen from the figure, the QPSO algorithm updates the global optimal position in iterations 3, 10 and 37, which implies that better learning rates are generated by QPSO algorithm in the iterations.

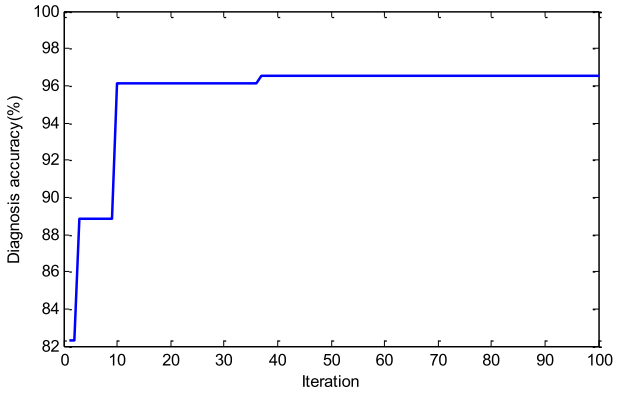

FIGURE 8. Learning rates' generation procedure of case 2 by using QPSO algorithm.

Adopting the generated learning rates, the DBN is used to extract features for each case. The input data are 100-dimensional, and features learnt by the first RBM and the second RBM are 50-dimensional and 25-dimensional, respectively. The features learnt by the second RBM are the features extracted by DBN. Kernel principal component analysis (KPCA) could produce principal components (PCs) from high-dimensional data, and it has been used in analog circuit fault diagnosis [15]. As a result, KPCA is employed to reduce the dimension of the input data and the features extracted by the DBN's two RBMs for the purpose of visualizing the extract features' space distributions of two cases.

The first 2 PCs including PC1 and PC2 of the input data, the first and second RBMs' extracted features of case 1 are generated by KPCA and showed in Fig. 9(a), Fig. 9(b), and Fig. 9(c), respectively. As can be seen from Fig. 9(a), there is obvious overlapping for F0, F1, F2 and F8 incipient fault classes. F3 and F5 incipient fault classes, and F4 and F6 incipient fault classes are respectively overlapped, which manifests that it is difficult to correctly classify every incipient fault class based on the input data. Meanwhile, F3 and F5 incipient fault classes, and F4 and F6 incipient fault classes are respectively overlapped in Fig.9(b). Finally, it shall be observed from Fig. 9(c) that all incipient fault classes are distinct ambiguity groups.

The first 2 PCs including PC1 and PC2 of the input data, the first and second RBMs' extracted features of case 2 are generated and showed in Fig. 10(a), Fig. 10(b), and Fig. 10(c), respectively. As can be seen from Fig. 10(a), there is obvious overlapping for F0, F2, F5, F6 and F7 incipient fault classes. Meanwhile, there is serious overlapping for F4, F8 and F12 incipient fault classes. As a result, it is very hard to correctly identify every incipient fault class based on the input data. As can be observed from Fig. 10(b), F2, F5, F7 and F9 incipient fault classes, F3, F9 and F11 incipient fault classes, and F8 and F12 incipient fault classes are overlapped, respectively. Finally, it can be observed from Fig. 10(c) that only F8 and F12 incipient fault classes are overlapped.

Based on the visualization effect of scatter plots in Figs. 9 and 10, it can be easily learn that the separability of each incipient fault class's features extracted by the proposed

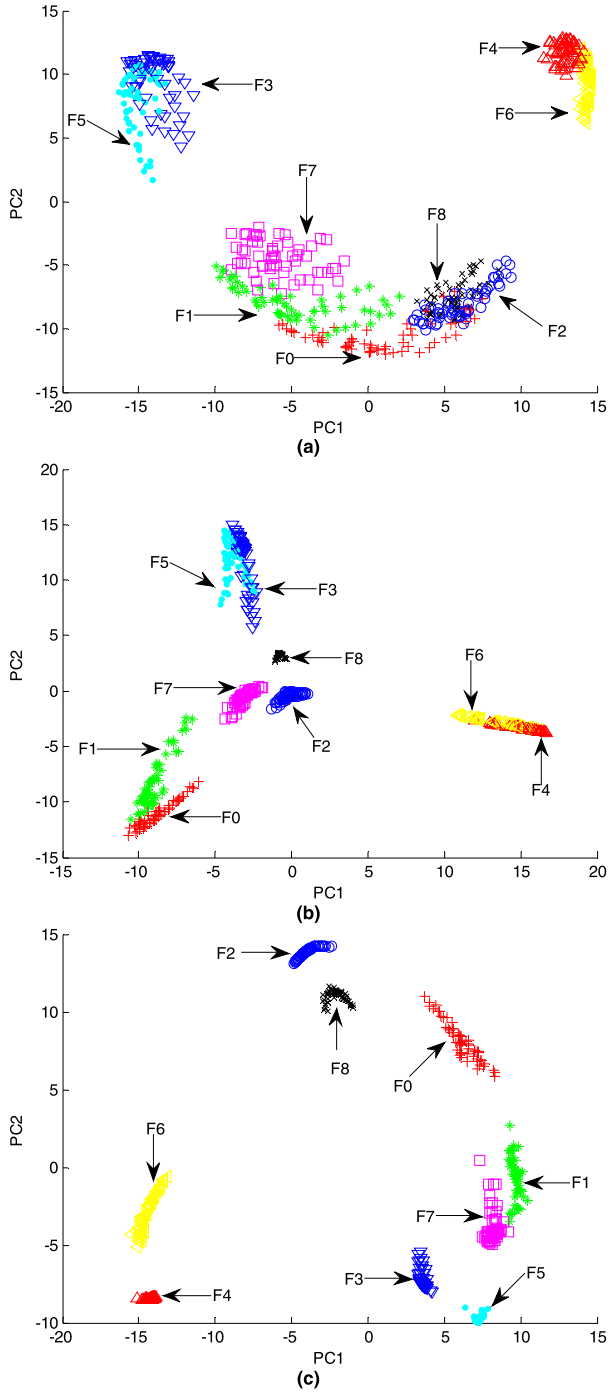

FIGURE 9. Two-dimensional scatter plots of incipient fault classes by using KPCA (a) input data (b) features learnt by the first RBM (c) features learnt by the second RBM.

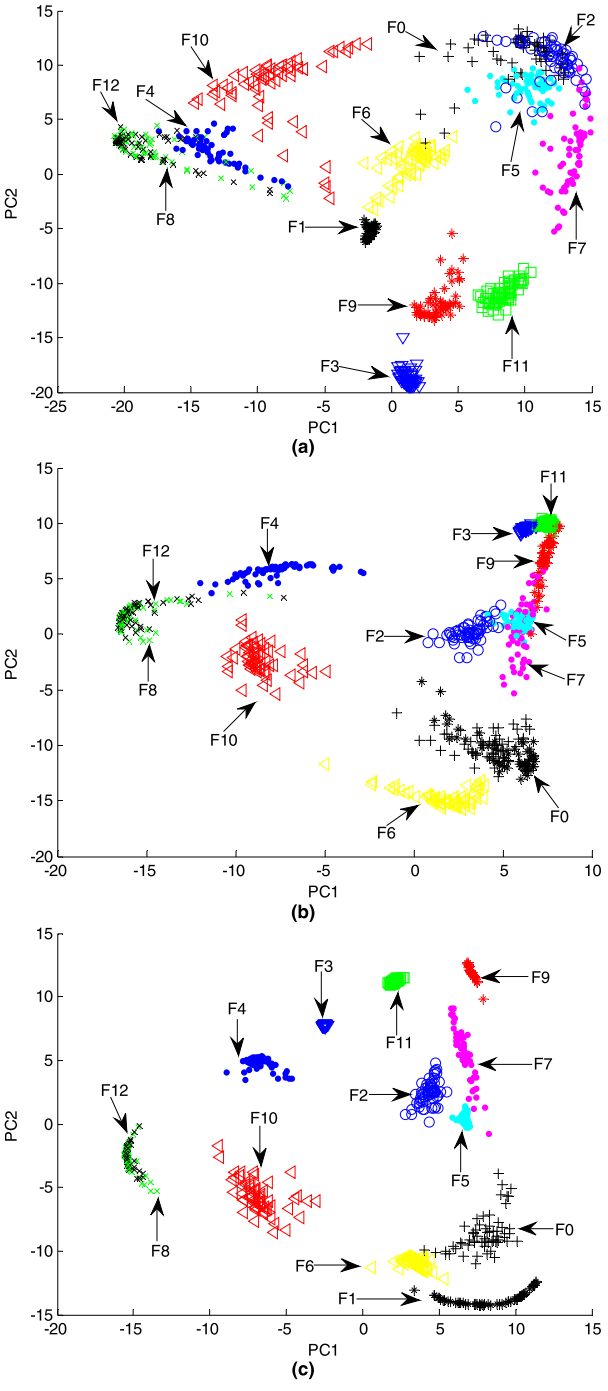

FIGURE 10. Two-dimensional scatter plots of incipient fault classes of case 2 by using KPCA (a) input data (b) features learnt by the first RBM (c) features learnt by the second RBM.

DBN is further enlarged compared to that of the input data, and the scatter plots of features extracted by the proposed DBN are more concentrated than that of the input data. This reveals that the proposed DBN method can extract deep and intrinsic features from the input data, and different incipient fault classes can be well separated, which is helpful to the successive classifier.

Based on the efficient features extracted by using the proposed DBN, a SVM based diagnosis model is constructed to identify different incipient faults. In order to improve the performance of SVM, QPSO algorithm is used to generate the regularization parameter and width factor for the SVM on basis of the extracted features. The QPSO algorithm's swarm size and the maximum iteration are set to 10 and 100,

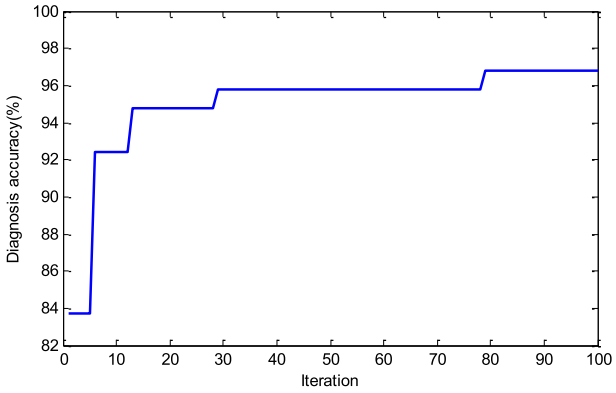

FIGURE 11. Regularization parameter and width factor generation procedure of case 2 by using QPSO algorithm.

TABLE 4. The two cases' regularization parameters and width factors generated by QPSO algorithm.

Case	Regularization parameter	Width factor
Case1	837.4185	9.2297
Case2	100.1249	0.0109

respectively; the contraction expansion coefficient decreases from 1 to 0.3 with the iteration. When the diagnosis accuracy reaches 100% or the iteration reaches its maximum in the training phase, the generation procedure is terminated.

Table 4 shows the generated regularization parameter and width factor of SVM in the two cases. The generation procedure of case 1 is only one iteration for the diagnosis accuracy reaches 100% in the first iteration. The generation procedure of case 2 is demonstrated in Fig. 11. As can be seen from the figure, the QPSO algorithm updates the global optimal position in iterations 6, 13, 29 and 79, which represents that better regularization parameter and width factor are produced in the iterations. At last, the QPSO algorithm outputs the best solution for the SVM.

Adopting the generated regularization parameter and width factor, an incipient fault diagnosis model on basis of SVM is constructed. Based on the testing data, the diagnosis accuracy of case 1 is 100% in the test phase, and the reason is that all incipient fault classes are well separated by the proposed DBN method. The diagnosis accuracy of each incipient fault class of case 2 is showed in Table 5. F0, F1, F2, F3, F5, F6, F7, F8, F11, F13 and F14 incipient fault classes are correctly classified. Meanwhile, 60 test data of F8 incipient fault class are correctly classified 49 times and misclassified as F12 incipient fault class 11 times; 60 test data of F12 incipient fault class are correctly classified 43 times and misclassified as F8 incipient fault class 17 times. The overall diagnosis accuracy is 96.41%.

D. COMPARISONS

In our work, a DBN method with learning rates generated by QPSO algorithm is presented to extract features. With respect

TABLE 5. Accuracy of each incipient fault class of the case 2.

Incipient fault code	Incipient fault class	Accuracy
F0	NF	100%
F1	$R_1\uparrow$	100%
F2	$R_1\downarrow$	100%
F3	$R_2\uparrow$	100%
F4	$R_2\downarrow$	100%
F5	$R_3\uparrow$	100%
F6	$R_3\downarrow$	100%
F7	$R_4\uparrow$	100%
F8	$R_4\downarrow$	81.7%
F9	$C_1\uparrow$	100%
F10	$C_1\downarrow$	100%
F11	$C_2\uparrow$	100%
F12	$C_2\downarrow$	71.7%

to the traditional DBN, its learning rates are set in the range of 0.01 and 0.5 according to experience. In order to validate the proposed DBN's performance in terms of features extraction, comparison simulations are designed. The traditional DBN respectively adopts 0.01, 0.02, 0.05, 0.1, 0.2 and 0.5 as the learning rates, and then extracts features based on the input data of case 2. After extraction, the extracted features' first 2 PCs including PC1 and PC2 generated by KPCA are displayed in Fig. 12. In Fig. 12(a), 0.01 is used as the learning rates of DBN. F0 and F6 incipient fault classes are slightly overlapped. Meanwhile, F2, F3 and F5 incipient fault classes are obviously overlapped, and F8 and F12 incipient fault classes are seriously overlapped. In Fig. 12(b), 0.02 is used as the learning rates of DBN. F2 and F5 incipient fault classes are overlapped, and F8 and F12 incipient fault classes are seriously overlapped. In Fig. 12(c), 0.05 is used as the learning rates of DBN. F0 and F6 incipient fault classes, F2 and F5 incipient fault classes, and F3 and F11 incipient fault classes are obviously overlapped, respectively. Meanwhile, F8 and F12 incipient fault classes are seriously overlapped. In Fig. 12(d), 0.1 is used as the learning rates of DBN. F1 and F6 incipient fault classes, and F3 and F7 incipient fault classes are obviously overlapped, respectively. Meanwhile, F2 and F5 incipient fault classes, and F8 and F12 incipient fault classes are seriously overlapped, respectively. In Fig. 12(e), 0.2 is used as the learning rates of DBN. F1 and F6 incipient fault classes, F2 and F5 incipient fault classes, and F3 and F7 incipient fault classes are obviously overlapped, respectively. Meanwhile, F8 and F12 incipient fault classes are seriously overlapped. In Fig. 12(f), 0.5 is used as the learning rates of DBN. F1 and F6 incipient fault classes, F2 and F5 incipient fault classes, and F3 and F7 incipient fault classes are obviously overlapped, respectively. Meanwhile, F8 and F12 incipient fault classes are seriously overlapped.

It can be easily seen that the numbers of overlapped incipient fault classes in Fig. 12(a), Fig. 12(b), Fig. 12(c), Fig. 12(d), Fig. 12(e) and Fig. 12(f) are all more than that in Fig. 10(c). Meanwhile, the separability of scatter plots of each incipient fault class in Fig. 10(c) is further enlarged compared to that in Fig. 12(a), Fig. 12(b), Fig. 12(c), Fig. 12(d), Fig. 12(e) and Fig. 12(f). Therefore, the groups of features

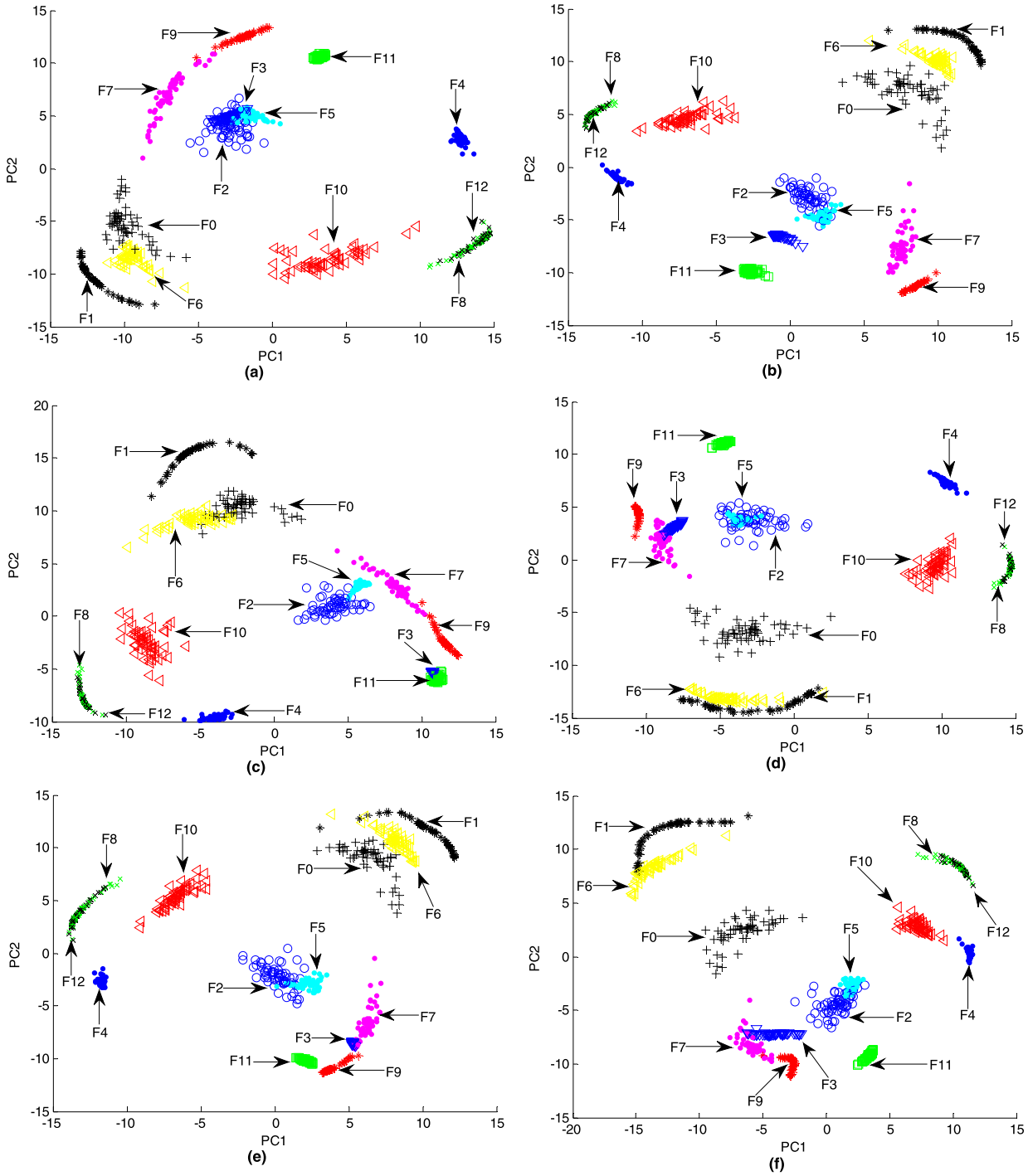

FIGURE 12. Two-dimensional scatter plots of incipient fault classes by using KPCA with different RBM's learning rate (a) 0.01, (b) 0.02, (c) 0.05, (d) 0.1, (e) 0.2 and (f) 0.5 of case 2.

extracted by using the proposed DBN are clearer and much better from the classification point of view than that by using the traditional DBN. It can be concluded that generating learning rates by using QPSO algorithm is very beneficial to improving DBN's features extraction performance.

For the purpose of validating the diagnosis performance of the proposed incipient fault diagnosis method, the proposed diagnosis method is compared with the typical analog circuit fault diagnosis methods in works [12], [14], [16], [17], [23]. In work [12], wavelet transform is employed as features extraction method, and back propagation neural network (BPNN) is used as diagnosis tool. In work [14], kurtosis and entropy of measured signal data are used as features, and BPNN serves as diagnosis tool. In work [16], wavelet

TABLE 6. Features extraction and diagnosis tools in the comparative works.

Method	Features extraction method	Diagnosis tool
Method in work [12]	Wavelet transform	BPNN
Method in work [14]	Kurtosis and entropy	BPNN
Method in work [16]	Wavelet transform	LRN
Method in work [17]	Wavelet transform	SVM
Method in work [23]	Wavelet-based fractal analysis	LSSVM

TABLE 7. Diagnosis accuracies of our method and the referenced methods.

Method	Case 1	Case 2
Method in work [12]	99.07%	92.95%
Method in work [14]	100%	94.87%
Method in work [16]	100%	95.51%
Method in work [17]	100%	95.90%
Method in work [23]	100%	95.00%
Method in our work	100%	96.41%

transform is utilized as features extraction method, and then linear ridgelet network (LRN) is used to identify analog circuit faults. In work [17], wavelet transform is employed as features extraction method, and then SVM is applied to classify analog circuit faults. In work [23], wavelet fractal dimensions of measured signal data serve as features, and then LSSVM is employed to recognize analog circuit faults. The features extraction methods and diagnosis tools of the typical analog circuit fault diagnosis methods are showed in Table 6.

The measured signal data of two cases are used to test the five typical diagnosis methods, where the comparison simulations are conducted under the same simulation conditions. The diagnosis results of five typical diagnosis methods are showed in Table 7. From the results of the table, it can be observed that diagnosis accuracy produced by method using wavelet transform and BPNN in work [12] is the lowest. The diagnosis accuracies produced by methods in works [16] and [17] are both improved because the works respectively employ LRN and SVM as diagnosis tools, which manifests that a better diagnosis tool can improve the classification performance obviously. Meanwhile, diagnosis accuracy produced by method in work [14] is also improved because the work adopts kurtosis and entropy as features, which reflects that an efficient features extraction method could enhance the diagnosis performance. Diagnosis accuracy of case 2 produced by method in work [23] is not very high for the advantage of wavelet fractal analysis is low computation, rather than extracting essential features. Because the proposed DBN based features extraction method can learn deep and intrinsic features from the measured data, the highest diagnosis accuracy is produced in our work.

VI. CONCLUSIONS

In this work, a novel analog circuit incipient fault diagnosis method using DBN based features extraction has been proposed. In the diagnosis scheme, DBN method has been used to extract the deep and intrinsic features from the measured time responses, where the learning rates of DBN have been produced by using QPSO algorithm. A SVM based incipient fault diagnosis model is set up to classify different incipient fault classes, where the SVM's parameters have also been generated by using QPSO algorithm. Through comparing the 2-dimensional scatter plots of incipient fault classes, the proposed DBN method can generate fewer overlapped incipient fault classes and greater separability than the traditional DBN method. Comparisons' results have verified that the proposed diagnosis method can produce higher diagnosis accuracy than other typical analog circuit fault diagnosis methods.

REFERENCES

[1] H. Hoang, S. Lee, Y. Kim, Y. Choi, and F. Bien, "An adaptive technique to improve wireless power transfer for consumer electronics," *IEEE Trans. Consum. Electron.*, vol. 58, no. 2, pp. 327–332, May 2012.

[2] X. Hu, S. J. Moura, N. Murgovski, B. Egardt, and D. Cao, "Integrated optimization of battery sizing, charging, and power management in plug-in hybrid electric vehicles," *IEEE Trans. Control Syst. Technol.*, vol. 24, no. 3, pp. 1036–1043, May 2016.

[3] C. Zou, C. Manzie, and D. Nešić, "A framework for simplification of PDE-based lithium-ion battery models," *IEEE Trans. Control Syst. Technol.*, vol. 24, no. 5, pp. 1594–1609, Sep. 2016.

[4] X. Hu, C. M. Martinez, and Y. Yang, "Charging, power management, and battery degradation mitigation in plug-in hybrid electric vehicles: A unified cost-optimal approach," *Mech. Syst. Signal Process.*, vol. 87, pp. 4–16, Mar. 2017.

[5] C. Zou, C. Manzie, D. Nešić, and A. G. Kallapur, "Multi-time-scale observer design for state-of-charge and state-of-health of a lithium-ion battery," *J. Power Sources*, vol. 335, pp. 121–130, Dec. 2016.

[6] S. Arias-Guzmán *et al.*, "Analysis of voltage sag severity case study in an industrial circuit," *IEEE Trans. Ind. Appl.*, vol. 53, no. 1, pp. 15–21, Jan./Feb. 2017.

[7] F. Li and P.-Y. Woo, "Fault detection for linear analog IC-the method of short-circuit admittance parameters," *IEEE Trans. Circuits Syst. I, Fundam. Theory Appl.*, vol. 49, no. 1, pp. 105–108, Jan. 2002.

[8] R. Spina and S. Upadhyaya, "Linear circuit fault diagnosis using neuromorphic analyzers," *IEEE Trans. Circuits Syst. II, Analog Digit. Signal Process.*, vol. 44, no. 3, pp. 188–196, Mar. 1997.

[9] F. Aminian and M. Aminian, "Fault diagnosis of analog circuits using Bayesian neural networks with wavelet transform as preprocessor," *J. Electron. Test.*, vol. 17, no. 1, pp. 29–36, Feb. 2001.

[10] M. Aminian and F. Aminian, "A modular fault-diagnostic system for analog electronic circuits using neural networks with wavelet transform as a preprocessor," *IEEE Trans. Instrum. Meas.*, vol. 56, no. 5, pp. 1546–1554, Oct. 2007.

[11] M. Aminian and F. Aminian, "Neural-network based analog-circuit fault diagnosis using wavelet transform as preprocessor," *IEEE Trans. Circuits Syst. II, Analog Digit. Signal Process.*, vol. 47, no. 2, pp. 151–156, Feb. 2000.

[12] F. Aminian, M. Aminian, and H. W. Collins, "Analog fault diagnosis of actual circuits using neural networks," *IEEE Trans. Instrum. Meas.*, vol. 51, no. 3, pp. 544–550, Jun. 2002.

[13] Y. Tan, Y. Sun, and X. Yin, "Analog fault diagnosis using S-transform preprocessor and a QNN classifier," *Measurement*, vol. 46, no. 7, pp. 2174–2183, Aug. 2013.

[14] L. Yuan, Y. He, J. Huang, and Y. Sun, "A new neural-network-based fault diagnosis approach for analog circuits by using kurtosis and entropy as a preprocessor," *IEEE Trans. Instrum. Meas.*, vol. 59, no. 3, pp. 586–595, Mar. 2010.

[15] Y. Xiao and L. Feng, "A novel linear ridgelet network approach for analog fault diagnosis using wavelet-based fractal analysis and kernel PCA as preprocessors," *Measurement*, vol. 45, no. 3, pp. 297–310, Apr. 2012.

[16] Y. Xiao and Y. He, "A linear ridgelet network approach for fault diagnosis of analog circuit," *Sci. China Inf. Sci.*, vol. 53, no. 11, pp. 2251–2264, Nov. 2010.
[17] P. Chen, L. Yuan, Y. He, and S. Luo, "An improved SVM classifier based on double chains quantum genetic algorithm and its application in analogue circuit diagnosis," *Neurocomputing*, vol. 211, pp. 202–211, Oct. 2016.
[18] D. Grzechca and J. Rutkowski, "Fault diagnosis in analog electronic circuits—The SVM approach," *Metrol. Meas. Syst.*, vol. 16, no. 4, pp. 583–598, Dec. 2009.
[19] J. Cui and Y. Wang, "A novel approach of analog fault classification using a support vector machines classifier," *Metrol. Meas. Syst*, vol. 17, no. 4, pp. 561–581, Dec. 2010.
[20] C. Zhang, Y. He, L. Yuan, W. He, S. Xiang, and Z. Li, "A novel approach for diagnosis of analog circuit fault by using GMKL-SVM and PSO," *J. Electron. Test.*, vol. 32, no. 5, pp. 531–540, Oct. 2016.
[21] J. Cui and Y. Wang, "Analog circuit fault classification using improved one-against-one support vector machines," *Metrol. Meas. Syst*, vol. 18, no. 4, pp. 569–582, Dec. 2011.
[22] R. Sałat and S. Osowski, "Support vector machine for soft fault location in electrical circuits," *J. Intell. Fuzzy Syst.*, vol. 22, no. 1, pp. 21–31, Jan. 2011.
[23] C. Zhang, Y. He, L. Zuo, J. Wang, and W. He, "A novel approach to diagnosis of analog circuit incipient faults based on KECA and OAO LSSVM," *Metrol. Meas. Syst.*, vol. 22, no. 2, pp. 251–262, Jun. 2015.
[24] L. Xu, J. Huang, H. Wang, and B. Long, "A novel method for the diagnosis of the incipient faults in analog circuits based on LDA and HMM," *Circuits, Syst. Signal Process.*, vol. 29, no. 4, pp. 577–600, Aug. 2010.
[25] B. Long, W. Xian, M. Li, and H. Wang, "Improved diagnostics for the incipient faults in analog circuits using LSSVM based on PSO algorithm with Mahalanobis distance," *Neurocomputing*, vol. 133, pp. 237–248, Jun. 2014.
[26] G. E. Hinton and R. R. Salakhutdinov, "Reducing the dimensionality of data with neural networks," *Science*, vol. 313, no. 5786, pp. 504–507, Jul. 2006.
[27] H. Lee, R. Grosse, R. Ranganath, and A. Y. Ng, "Unsupervised learning of hierarchical representations with convolutional deep belief networks," *Commun. ACM*, vol. 54, no. 10, pp. 95–103, Oct. 2011.
[28] A. R. Mohamed, T. N. Sainath, G. Dahl, B. Ramabhadran, G. E. Hinton, and M. A. Picheny, "Deep belief networks using discriminative features for phone recognition," in *Proc. ICASSP*, Prague, Czech Republic, 2011, pp. 5060–5063.
[29] Y. Chen, X. Zhao, and X. Jia, "Spectral-spatial classification of hyperspectral data based on deep belief network," *IEEE J. Sel. Topics Appl. Earth Observ. Remote Sens.*, vol. 8, no. 6, pp. 2381–2392, Jun. 2015.
[30] C. Cortes and V. Vapnik, "Support-vector networks," *Mach. Learn.*, vol. 20, no. 3, pp. 273–297, Sep. 1995.
[31] J. Sun, W. Fang, X. Wu, V. Palade, and W. Xu, "Quantum-behaved particle swarm optimization: Analysis of individual particle behavior and parameter selection," *Evol. Comput.*, vol. 20, no. 3, pp. 349–393, Jul. 2012.
[32] R. Eberhart and J. Kennedy, "A new optimizer using particle swarm theory," in *Proc. MHS*, Nagoya, Japan, 1995, pp. 39–43.
[33] L. Lin, F. Guo, X. Xie, and B. Luo, "Novel adaptive hybrid rule network based on TS fuzzy rules using an improved quantum-behaved particle swarm optimization," *Neurocomputing*, vol. 149, pp. 1003–1013, Feb. 2015.
[34] W. Fang, J. Sun, X. Wu, and V. Palade, "Adaptive Web QoS controller based on online system identification using quantum-behaved particle swarm optimization," *Soft Comput.*, vol. 19, no. 6, pp. 1715–1725, Jun. 2015.
[35] S. Zhang, Y. Zhang, and J. Zhu, "Rolling element-bearing feature extraction based on combined wavelets and quantum-behaved particle swarm optimization," *J. Mech. Sci. Technol.*, vol. 29, no. 2, pp. 605–610, Feb. 2015.
[36] A. S. S. Vasan, B. Long, and M. Pecht, "Diagnostics and prognostics method for analog electronic circuits," *IEEE Trans. Ind. Electron.*, vol. 60, no. 11, pp. 5277–5291, Nov. 2013.

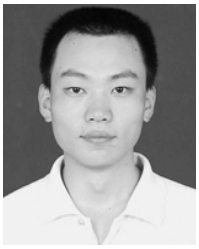

CHAOLONG ZHANG received the Ph.D. degree from the Hefei University of Technology in 2018. He is currently an Associate Professor with the School of Physics and Electronic Engineering, Anqing Normal University. He is also a Post-Doctoral Researcher in electrical engineering with Wuhan University. His current research interests include fault diagnostics and prognostics of analog and mixed-signal circuits, and battery capacity prognostic.

YIGANG HE received the Ph.D. degree from Xi'an Jiaotong University in 1996. He is currently a Professor and a Doctoral Supervisor with the School of Electrical Engineering, Wuhan University. He is one of winners of the National Distinguished Young Scientists Foundation. His research interests are in the areas of circuit theory and its applications, testing and fault diagnosis of analog and mixed-signal circuits, smart grid, radio frequency identification technology, and intelligent signal processing.

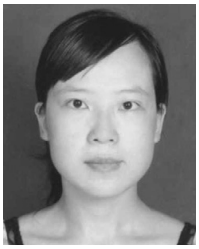

LIFENG YUAN received the Ph.D. degree in electrical engineering from Hunan University, China, in 2011. She is currently a Professor with the School of Electrical Engineering and Automation, Hefei University of Technology, China. Her research interests are in the area of test theory for circuit and system.

SHENG XIANG received the M.Sc. degree from the Hefei University of Technology in 2014, where he is currently pursuing the Ph.D. degree. His research interests are applications, testing and fault diagnosis of power electronic system.